Supplementary Materials

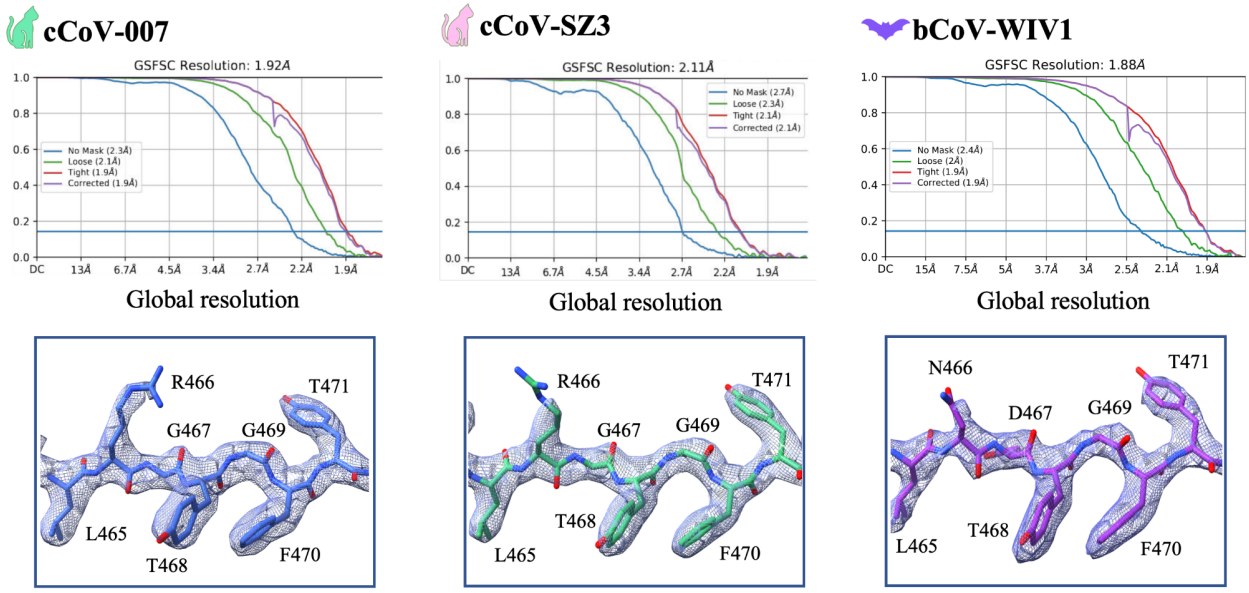

Supplementary figure 1. Comparison of reconstruction resolutions and map quality between SARSr-CoV glycoproteins. *(Top)* Gold-standard Fourier shell correlation plots are computed within cryoSPARC from two independent half-maps and report a global resolution for each reconstruction. *(Bottom)* Amino acid residues contained within the receptor binding motif loop (L465-T471) are presented within the electron density, set to a standard deviation threshold of 0.25 in all panels.

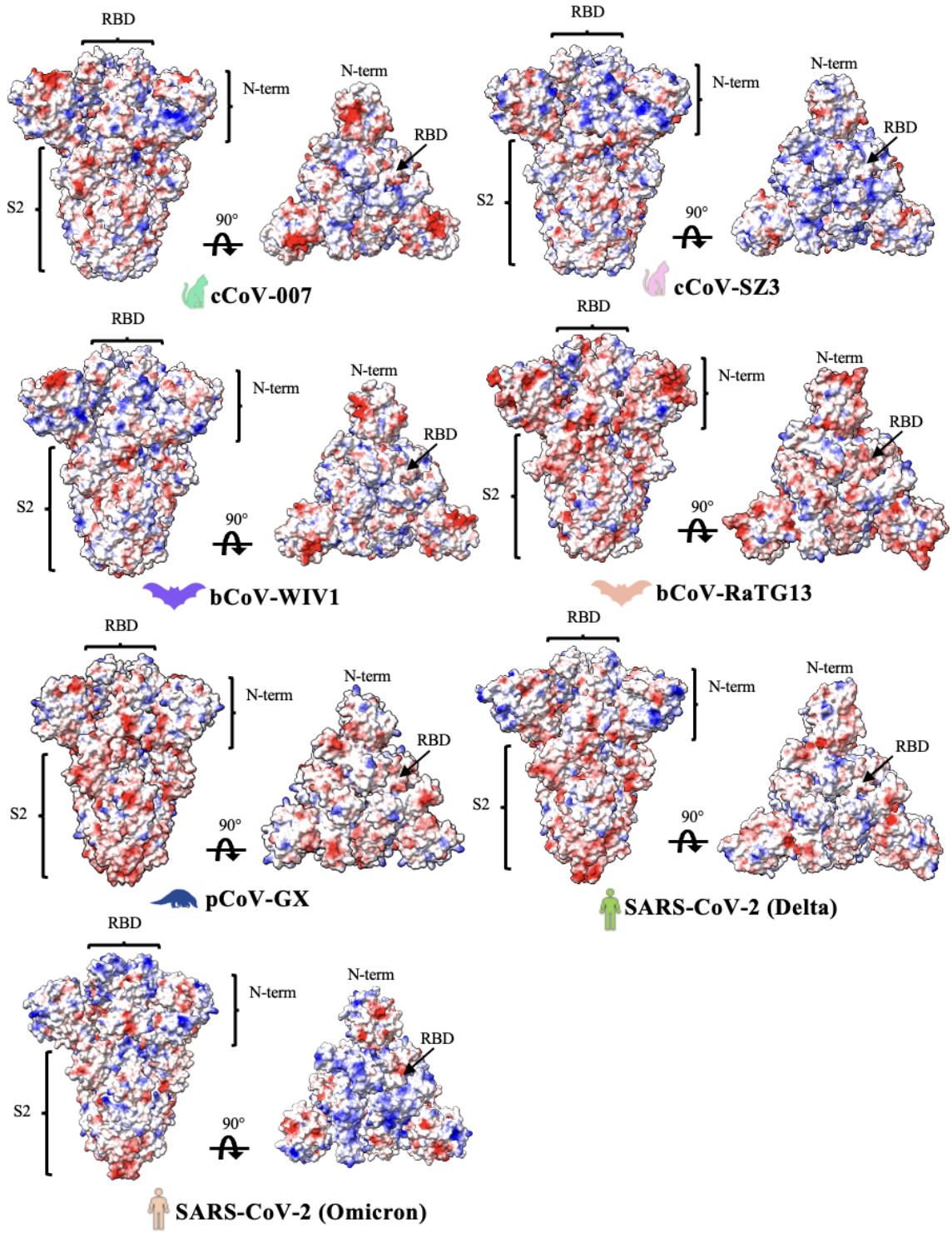

Supplementary figure 2. Coulombic electrostatic potential of SARSr-CoV glycoproteins. Molecular surface representation of side and top views of SARSs-CoV spike proteins are coloured by Coulumbic electrostatic potential calculated in UCSF ChimeraX according to Coulumbs law: $\varphi = \Sigma [q_i / (\varepsilon d_i)]$. Negative potential is coloured blue and positive potential is coloured red. The SARS-CoV-2 Wuhan-Hu-1 (PDB: 7E7B) and Omicron spikes (PDB: 7EWK), as well as SARSr-CoV spikes pCoV-GX (PDB: 7BBH) and bCoV-RaTG13 spike (PDB: 7CN4) were downloaded from the Protein Data Bank.

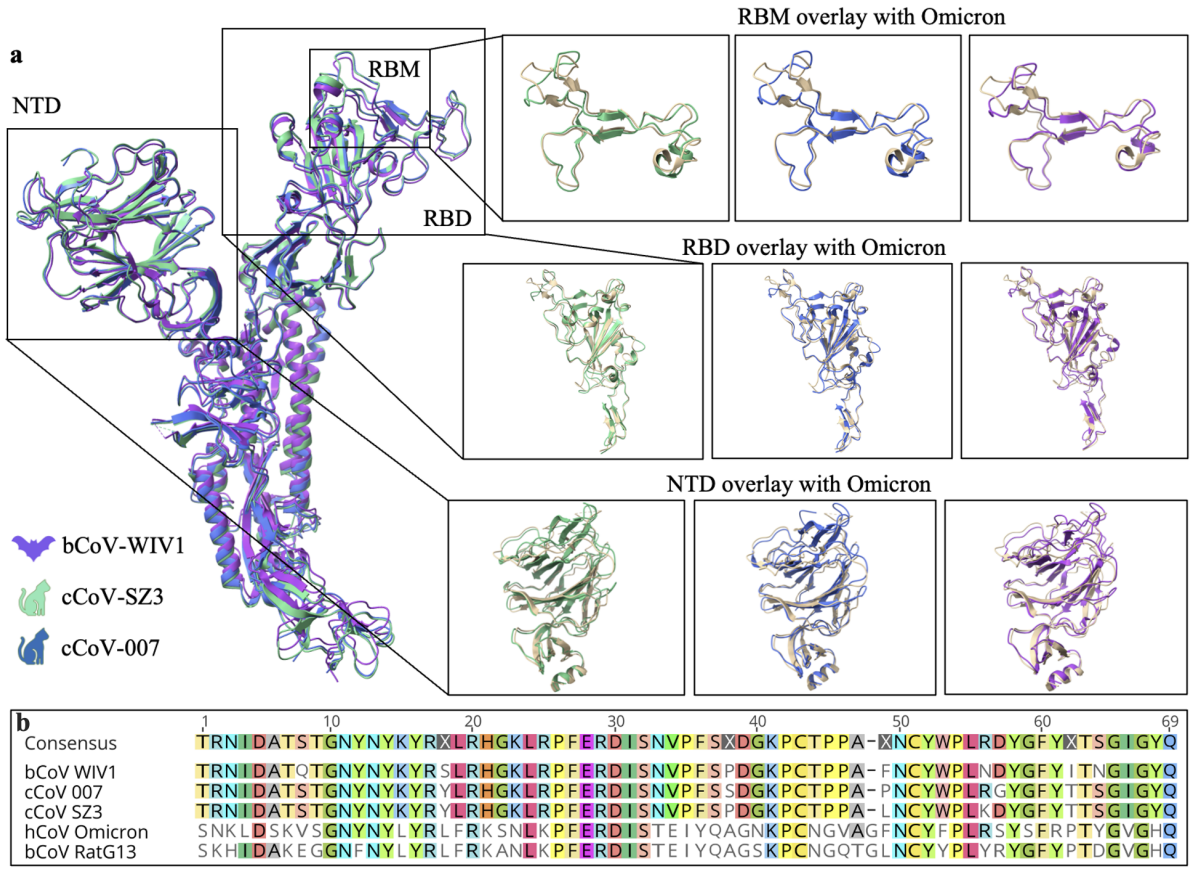

Supplementary figure 3. Structural and sequence based comparison of S1 domains between SARSr-CoV spike glycoprotein and Omicron. a, Alignment of glycoprotein monomer cCoV SZ3 (green), cCoV 007 (blue) and bCoV WIV1 (purple), followed by alignments of the receptor binding motif (RBM), receptor binding domain (RBD) and the N-Terminal domain (NTD) of novel glycoprotein structures against omicron (PDB 7WK2). **b,** Geneious global sequence alignment of RBM from 6 spike glycoproteins, bCoV-WIV1, cCoV-SZ3, cCoV-007, human (h) CoV Omicron, bCoV RaTG13 and pangolin (p) CoV GX (PDB: 7BBH).

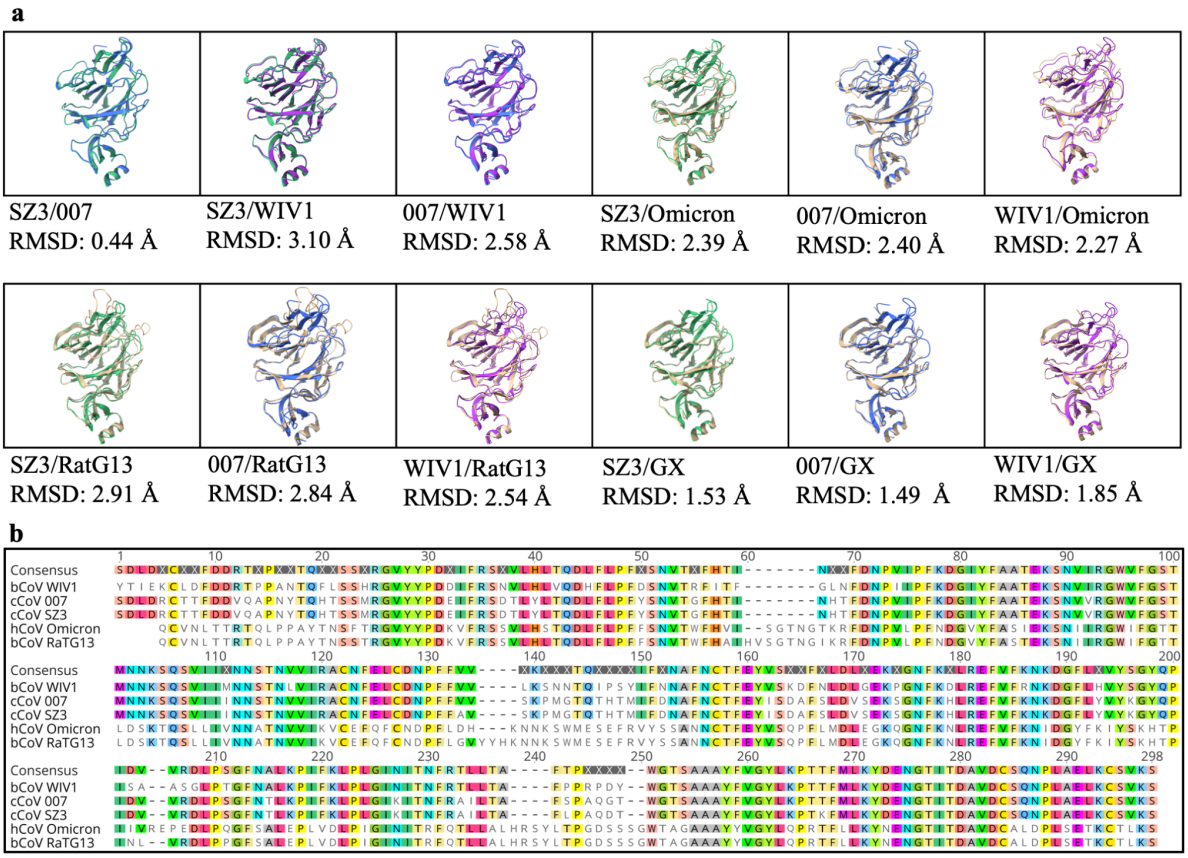

Supplementary figure 4. Structural and sequence based comparison of N-terminal domain between SARSr-CoV spike glycoproteins. a, Alignment and RMSD calculation of N-terminal domains (NTD) from civet (c) CoV-SZ3 shown in green, cCoV-007 shown in blue, bat (b) CoV-WIV1 shown in purple. Human (h) Omicron (PDB: 7WK2), bCoV-RaTG13 (PDB: 7CN4), pangolin (p) CoV-GX (PDB: 7BBH) all shown in tan. RMSD values calculated using unpruned atom pairs **b**, Geneious global sequence alignment of NTDs from 6 spike glycoproteins, bCoV-WIV1, cCoV-SZ3, cCoV-007, hCoV Omicron, bCoV RaTG13 and pCoV GX (PDB: 7BBH).

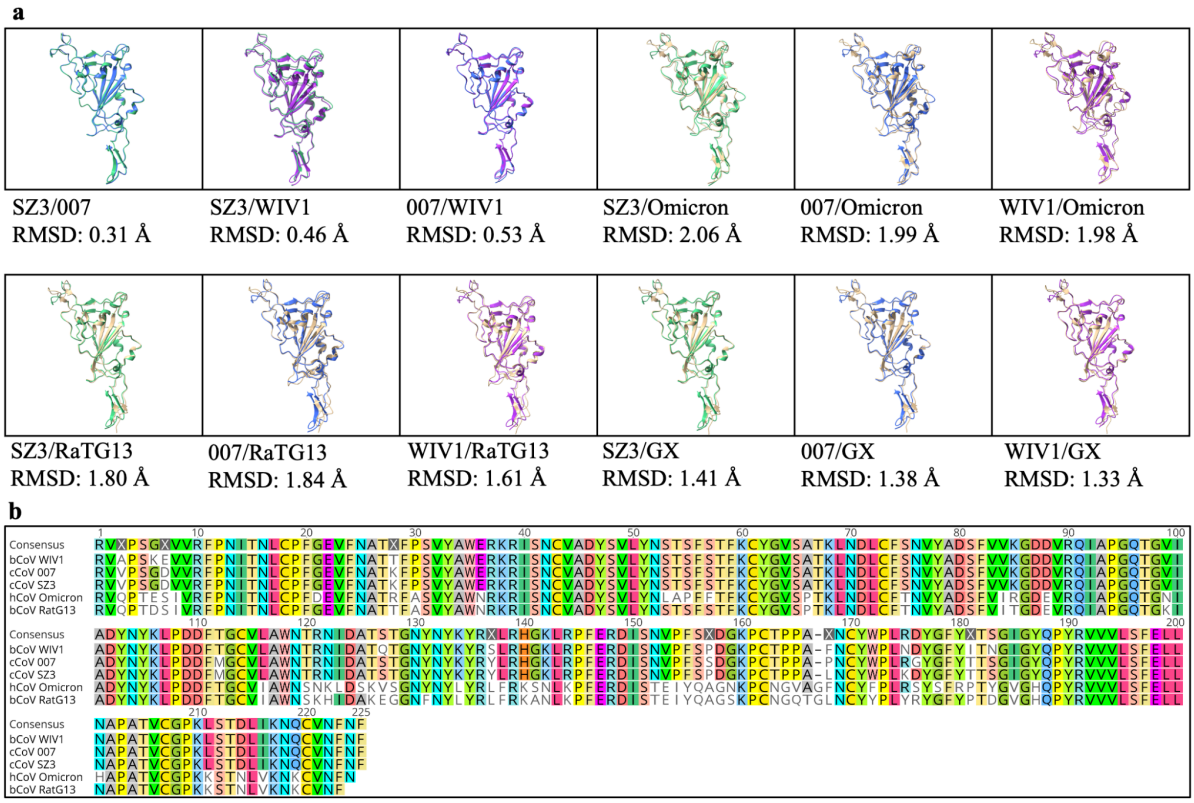

Supplementary figure 5. Structural and sequence based comparison of receptor binding domain between SARSr-CoV spike glycoproteins. a, Alignment and RMSD calculation of receptor binding domain (RBD) from civet (c) CoV-SZ3 shown in green, cCoV-007 shown in blue, bat (b) CoV-WIV1 shown in purple. Human (h) Omicron (PDB: 7WK2), bCoV-RaTG13 (PDB: 7CN4), pangolin (p) CoV-GX (PDB: 7BBH) all shown in tan. RMSD values calculated using unpruned atom pairs **b**, Geneious global sequence alignment of RBDs from 6 spike glycoproteins, bCoV-WIV1, cCoV-SZ3, cCoV-007, hCoV Omicron, bCoV RaTG13 and pCoV GX (PDB: 7BBH).

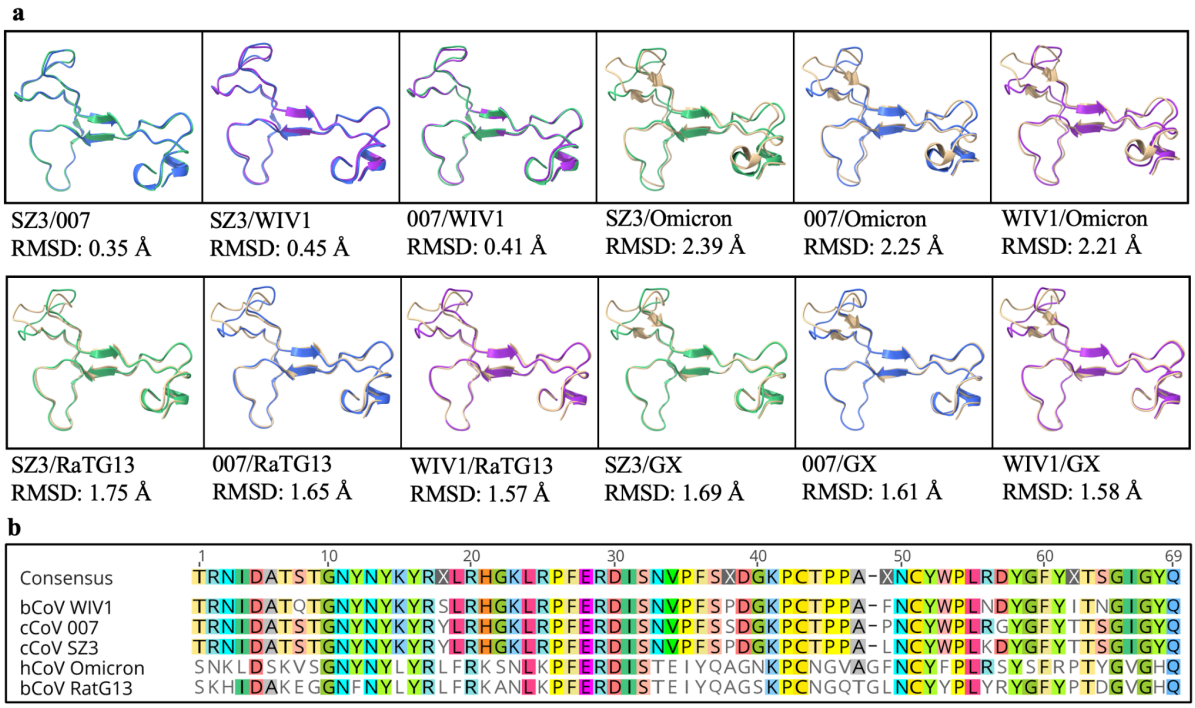

Supplementary figure 6. Structural and sequence based comparison of receptor binding motif between SARSr-CoV spike glycoproteins. a, Alignment and RMSD calculation of receptor binding motif (RBM) from civet (c) CoV-SZ3 shown in green, cCoV-007 shown in blue, bat (b) CoV-WIV1 shown in purple. Human (h) Omicron (PDB: 7WK2), bCoV-RaTG13 (PDB: 7CN4), pangolin (p) CoV-GX (PDB: 7BBH) all shown in tan. RMSD values calculated using unpruned atom pairs **b**, Geneious global sequence alignment of RBMs from 6 spike glycoproteins, bCoV-WIV1, cCoV-SZ3, cCoV-007, hCoV Omicron, bCoV RaTG13 and pCoV GX (PDB: 7BBH).

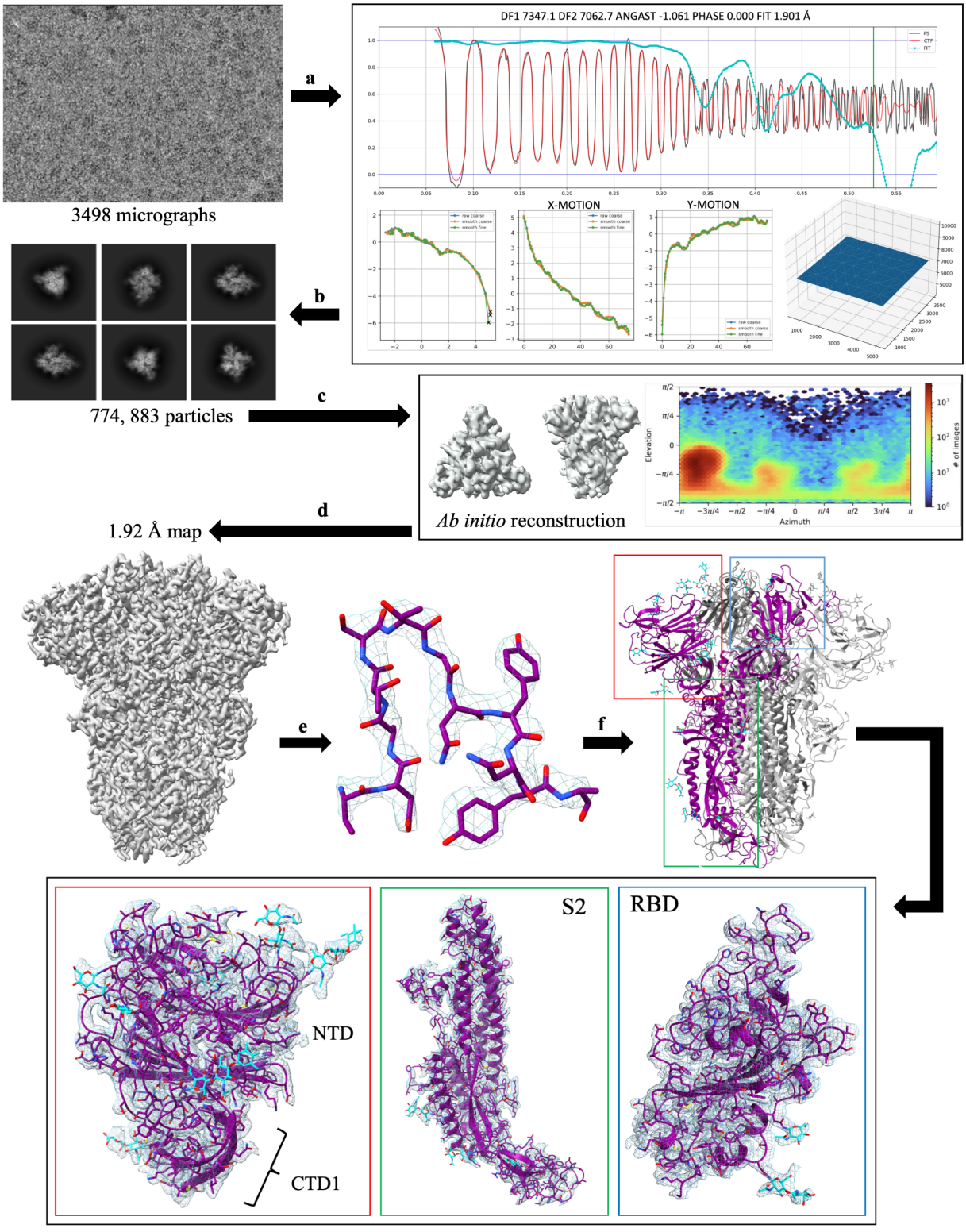

Supplementary figure 7. Image processing and reconstruction of cCoV-007 glycoprotein. (*a*) Data processing included patch-based motion correction and patch-based CTF correction. (*b*) Particles were picked by automated blob picking, extracted and classed to produce templates used in template-based particle picking. Following iterative 2D classing, 774,883 particles were selected for use in downstream reconstruction jobs. (*c*) Ab initio reconstruction produced an initial 3D model. (*d*) The initial model was refined in iterative homogeneous and non-uniform refinement jobs using the particle stack from (*b*) to produce a final model extending to a global atomic resolution of 1.92 Å. (*e*) An initial model was built using a reference model (PDB: 7E7B) and fit into the electron density using ISOLDE. (*d*) Refinement was performed using Stand-Alone Coot and Phenix.

Supplementary Table 1. Cryo-EM data collection, refinement and validation statistics for SARSs-CoV glycoproteins.

Data collection and processing	**cCoV-007**	**cCoV-SZ3**	**bCoV-WIV1**
Magnification	×105,000	×105,000	×130,000
Detector	K3 (gatan)	K3 (gatan)	K3 (gatan)
Voltage (kV)	300	300	300
Electron exposure (e /Å^2)	59	59	67
Spherical aberration (mm)	2.7	2.7	2.7
Defocus range (μm)	-0.6 – -2	-0.6 – -2	-0.6 – -2
Pixel size (Å/pix)	0.84	0.84	0.65
Frames	75	75	95
Symmetry imposed	C3	C3	C3
Initial particle images (no.)	>5,000,000	>3,000,000	>5,000,000
Final particle images (no.)	~775,000	~800,000	~800,000
Map resolution (Å)	1.92	2.11	1.88
Refinement			
Initial model used (PDB code)	*ab initio*	*ab initio*	*ab initio*
Model resolution (Å)	N/A	N/A	N/A
Map sharpening B factor (Å^2)	-46	-53	-41
Bond lengths (Å)	0.004	0.021	0.020
Bond angles (°)	0.662	2.23	2.187
Protein residues	3264	3261	3273
Validation			
MolProbity score	1.47	1.59	1.76
EMRinger score	5.76	5.76	4.77
Clashscore	3.49	2.79	4.92
Poor rotamers (%)	0 (0)	1.6	1.4
Ramachandran plot Favored (%) Allowed (%) Disallowed (%)	 94.63 2.19 0.9	 94.63 5.37 0	 94.22 5.71 0.06
Rama-Z (Ramachandran plot Z-score, RMSD) whole (N = 3240) helix (N = 675) sheet (N = 726) loop (N = 1839)	 0.06 (0.14) 2.06 (0.20) 0.30 (0.19) -0.86 (0.13)	 -3.08 (0.12) -2.21 (0.14) -2.60 (0.18) -1.78 (0.12)	 -2.66 (0.12) -2.49 (0.13) -1.45 (0.22) -1.60 (0.12)
C-beta outliers (%)	0.13	0.3	0.07